RESEARCH ARTICLE

NIMA-related kinase 1 (NEK1) regulates meiosis I spindle assembly by altering the balance between α-Adducin and Myosin X

Miguel A. Brieño-Enríquez*, Stefannie L. Moak, J. Kim Holloway, Paula E. Cohen

Department of Biomedical Sciences and Center for Reproductive Genomics, Cornell University, Ithaca, New York, United States of America

* mab587@cornell.edu

Abstract

NIMA-related kinase 1 (NEK1) is a serine/threonine and tyrosine kinase that is highly expressed in mammalian germ cells. Mutations in *Nek1* induce anemia, polycystic kidney and infertility. In this study we evaluated the role of NEK1 in meiotic spindle formation in both male and female gametes. Our results show that the lack of NEK1 provokes an abnormal organization of the meiosis I spindle characterized by elongated and/or multipolar spindles, and abnormal chromosome congression. The aberrant spindle structure is concomitant with the disruption in localization and protein levels of myosin X (MYO10) and α-adducin (ADD1), both of which are implicated in the regulation of spindle formation during mitosis. Interaction of ADD1 with MYO10 is dependent on phosphorylation, whereby phosphorylation of ADD1 enables its binding to MYO10 on mitotic spindles. Reduction in ADD1 protein in NEK1 mutant mice is associated with hyperphosphorylation of ADD1, thereby preventing the interaction with MYO10 during meiotic spindle formation. Our results reveal a novel regulatory role for NEK1 in the regulation of spindle architecture and function during meiosis.

Introduction

Meiosis is a specialized cell division characterized by a single round of DNA replication followed by two rounds of chromosome segregation, resulting in the formation of haploid gametes for sexual reproduction. At the first male meiotic division (MI), homologous (maternal and paternal) chromosomes must segregate equally into two daughter cells, each of which then undergoes a mitosis-like second meiotic division (MII) in which sister chromatids separate into the haploid gametes. In mammals, meiosis in males results in four haploid gametes, while meiosis in female results in one haploid gamete per meiosis, the remaining genetic material being distributed between two polar bodies. Regardless of the sex of the individual, in order to achieve accurate segregation at both divisions, tension must be established on the meiotic spindles and this is achieved by the formation of crossovers between homologous chromosomes in meiosis I, and by cohesion between sister chromatids in both meiosis I and meiosis II [1].

Cohesion is also necessary for sister kinetochore attachment to microtubules during meiotic spindle formation [2].

In eukaryotes, the microtubule spindle is the structure that orchestrates chromosome alignment and segregation during both mitotic and meiotic divisions [3]. In mitosis, the microtubules that compose the spindle are mostly nucleated from centrosomes, which act as a major microtubule organizing center (MTOC) [2–4]. Centrosomes are composed of pairs of centrioles surrounded by pericentriolar material (PCM) that posses microtubule nucleation activity. When mitosis starts, centrosomes separate to opposite sides of the nuclear envelope, defining the poles of the spindle and allowing the bipolar spindle [2,4]. However, there is a sexual dismorphism during the meiosis, where the male spindle behaves like a mitotic spindle, while in oocytes, the spindle it is formed without centrosomes [4,5]. Another important difference is the stringency of the spindle checkpoint in females, in which the oocyte still proceeds through the first meiotic division despite disruptions in the spindle and chromosome congression at metaphase plate [6]. Such differences in spindle dynamics in male and female mammals suggest that different regulatory proteins may predominate in each sex.

Several families of kinases such as Polo kinases, Aurora kinases and NEK kinases have been implicated in the regulation of cell cycle events in both mitosis and meiosis [7,8]. The founding member of the NEK family is the *Aspergillus nidulans* never-in-mitosis-gene-A (NIMA) protein [9]. NIMA is a serine/threonine kinase involved in the initiation of mitosis and in promoting chromosome condensation. Genetic ablation of NIMA results in cell cycle arrest at G2, while overexpression of *NIMA* leads to premature entry into mitosis [7]. In mammals, there are 11 orthologs of *NIMA* that comprise the NIMA-like (NEK) family of kinases. *Nek1* is unique in that it encodes both the serine/threonine kinase activity typical of the NEK family as well as tyrosine kinase activity that is not a feature of other NEKs [10]. NEK1 has been implicated in ciliogenesis [11] and DNA damage response [12–15]. Additionally, NEK1 is highly expressed in mouse germ cells [16], where it appears to play essential roles in meiosis I and possibly also at later stages [17,18].

The *Kat2J* allele of *NEK1* is a spontaneous point mutation within the coding sequence of *Nek1* that results in a premature stop codon leading to a truncated protein lacking the both kinase domains [16]. $Nek1^{kat2j/kat2j}$ mice display polycystic kidneys, dwarfism, anemia and male sterility [16,19]. Interestingly, while initial reports mention that $Nek1^{kat2j/kat2j}$ females had low fertility rates [16,19], in our animal facility females no pregnancies are observed [17] possibly reflecting subtle background effects among mouse strains. Our previous studies of meiosis in $Nek1^{kat2j/kat2j}$ mice showed that the loss of NEK1 activity induces aberrant retention of cohesin subunit Structural Maintenance of Chromosomes protein 3 (SMC3), at the end of meiotic prophase I [17]. More recently, we showed NEK1 regulates cohesin removal, in part, through regulation of wings apart-like homolog (WAPL) during meiotic prophase I [18], as part of the so-called Prophase pathway for cohesin removal. This regulation of WAPL by NEK1 is mediated through WAPL interactions with the cohesin-associated protein, PDS5 homolog B (PDS5B), and protein phosphatase 1 gamma (PP1γ), both of which also interact with NEK1 [18].

In the current study, and given the conserved function of NEK proteins in spindle assembly dynamics, we investigated the role of NEK1 downstream of prophase I events. Our results demonstrate that loss of NEK1 induces failure of meiotic spindle organization in both males and females, leading to elongated spindles, multipolar spindles, and abnormal chromosome congression. Concurrent with this, we observe altered levels and localization of two proteins known to regulate mitotic spindle dynamics: the unconventional myosin, myosin X (MYO10), and α-adducin (ADD1). Interaction of ADD1 with MYO10 is dependent on phosphorylation of ADD1 which allows for the interaction of these two proteins on mitotic spindles [20].

Depletion of ADD1 or changes in its phosphorylation status results in abnormal mitotic spindles [20]. Our studies demonstrate that loss of NEK1 kinase causes changes in MYO10 and ADD1 protein levels, and hyperphosphorylation and deamination of ADD1 caused at least in part by the abnormal function of PP1 during meiotic spindle formation. Interestingly spindle phenotypes seem not directly related to the role of NEK1 in prophase I events.

Material and methods

Mice and genotyping

All mouse studies were conducted with the prior approval of the Cornell Institutional Animal Care and Use Committee (Protocol 2010–0054). The mice were bred under pathogen-free, controlled temperature ($22 \pm 1°C$) and regulated humidity (50–55%) conditions with periods of light/dark of 12 h and food available ad libitum. Mice were euthanized using CO_2 administration method.

The $Nek1^{kat2j/kat2j}$ line was obtained originally from Jackson Laboratory (Bar Harbor, Maine), and has been established in our mouse colony for more than nine years. Genotyping of this mouse line was performed following the protocol described elsewhere [17]. For the purposes of these studies, male mice were 8 weeks old and female where used at 24–28 days old. Homozygous mutant animals of ($Nek1^{kat2J/kat2J}$) were compared with wild type ($Nek1^{+/+}$) littermates on a C57Bl/6J background.

Male and female spindle preparation

Male spindle analysis was performed in testis from 8 week old mice following the protocol described elsewhere [21,22]. Briefly, following euthanasia, the testes were removed, decapsulated and placed in PBS. Using fine forceps, tubules were separated and analysed under a stereomicroscope. Differential light absorption of the tubules creates different zones that can be defined by different cell populations [22]. The different zones are consequence of the paracrine regualtion by Sertoli cells, spermatogenesis proceeds in synchronized waves along the seminiferus tubules, and every given cross-section contains only certain cell types, that produces a diferent light absorbation creating zones [22]. These zones are the weak spot that correspond to the spermatogenic stages XII-I, the strong spot (stages II-VI), the dark zone (stages VII-VIII) and the pale zone (stage IX-XI) We selected the zone corresponding to the spermatogenetic development XI and XII that are rich in meiotic cells during both meiosis I and meiosis II. Tubules were placed in fresh PBS and these required zones were excised and placed on poly-lysine-coated slides (P4981, Thermo Fisher). Tubule sections were fixed for 10 minutes (1% paraformaldehyde and 0.15% Triton-X, pH 9.2) and then squashed under a coverslip. Slides with the squashed tubules were put into liquid nitrogen for 20 seconds and thereafter the coverslip removed and washed with PBS-0.4% Kodak Photo flo (Kodak) (3 times for 5 minutes each). Slides were kept at -80°C or stained immediately.

Female spindle analysis was performed with oocytes from 24–28 day old mice following our previously published protocol [23]. Briefly, after dissection, ovaries were collected in collection medium (Waymouths's medium (11220035, Gibco), 10% Fetal bovine serum (26140079, Gibco), 1% penicillin-streptomycin (P4333-100ML, Sigma-Aldrich) and 0.1% sodium pyruvate (11360070, Gibco)). Oocytes were released from ovarian follicles using 30-gauge needles, and oocytes with germinal vesicles placed in EmbryoMax KSOM medium (MR-121-D, EMD Millipore). Oocytes were cultured for 6hr in EmbryoMax KSOM medium drops at 37°C, 5% CO2. After incubation, oocytes were placed in fibrinogen-thrombin clot, incubated for 60 seconds at 37°C, and rinsed with 1XPBS containing 2% Triton-X (BP151-500, Fisher Scientific) for 3 min. Oocytes were fixed for 30 minutes at 37°C. Fixation was

followed by a 15 minute wash in 0.1% NGS (5 ml 10X PBS, 50 μL goat serum and 50 ml Milli-Q water). Oocytes were stored at 4˚C or stained immediately.

Spindle immunofluorescence staining

Male and female fixed spindles slides were washed in PBS containing 0.4%Kodak Photo flo (Kodak) for 5 min, followed by 0.1% PBS-Triton X and blocked in 1XPBS-antibody dilution buffer (ADB) before being incubated over night at 4˚C with the primary antibody. Primary antibodies used were: rabbit anti-ADD1 (GTX101600, Genetex. Dilution 1:100), rabbit anti-MYO10 (24565-1-AP, Proteintech. Dilution 1:100) and rabbit anti-β-tubulin (T8328, Sigma. Dilution 1:500). After overnight incubation, slides were washed to remove the unbound antibodies and incubate for 2 hours at 37˚C with Alexafluor™ secondary antibodies (Molecular Probes Eugene OR, USA). Slides were washed and mounted with Prolong Gold antifade (Molecular Probes). Image acquisition was performed using a Zeiss Imager Z1 microscope under 20X, 40X or 63X magnifying objectives, at room temperature. Images were processed using ZEN 2 (Carl Zeiss).

Mass spectrometry

Mass spectrometry was performed in the Cornell University Proteomics and Mass Spectrometry facility. 2D LC-MS/MS raw data files were acquired using Orbitrap Elite (Thermo Scientific). We performed a database search using Mascot searching against the SwissProt mouse database from Uniprot website (http://www.uniprot.org) using Mascot software version 2.3.02 (Matrix Science, UK). The default Mascot search settings were as follows: one missed cleavage site by trypsin allowed with fixed MMTS modification of cysteine, fixed four-plex iTRAQ modifications on Lys and N-terminal amines and variable modifications of methionine oxidation, deamidation of Asn and Gln residues, and 4-plex iTRAQ on Tyr for iTRAQ 4-plex analysis. One or two-missed cleavage site by trypsin allowed with fixed carboxamidomethyl modification of cysteine, fixed six-plex TMT modifications on Lys and N-terminal amines and variable modifications of methionine oxidation, deamidation of Asn and Gln residues, and 6-plex TMT on Tyr for TMT 6-plex analysis. The quantitative protein ratios were weighted and normalized by the median ratio with outlier removal set automatic in Mascot for each set of experiments. Only those proteins with ratios equivalents to two-fold increase or two-fold reduction were considered significant. To obtain the specific post-traslational modification of the peptides we perfumed TiO2 enrichment followed by the proteomics analysis as was described above.

Western blotting

Whole testis protein and oocyte protein were extracted by sonication in RIPA buffer. Samples were boiled for 5 min in sample buffer, electrophoresed on SDS-polyacrylamide gels (8%) and transferred to nitrocellulose membranes. Primary antibody incubation was performed overnight at 4˚C at 1:1000 dilution (antibodies are the same used in spindle staining). Incubation with secondary antibodies was performed for two hours at room temperature (secondary HRP conjugated antibodies were obtained from Pierce, Life Technologies). Signal-detection was carried out using the superSignal substrate (Thermo Scientific). Loading control was performed using GAPDH-HPR (PA1-987-HRP, from ThermoFisher). Images were captured with BIO RAD Image Lab 5.1and analyzed by ImageJ version 1.49v (http://rsbweb.nih.gov/ij).

Results

Loss of NEK1 induces abnormal meiotic spindle formation and failed chromosome congression at the first meiotic division in males and females

We analyzed the role of NEK1 in spindle formation and chromosome orientation at MI in oocytes and spermatocytes from $Nek1^{+/+}$ and $Nek1^{kat2j/kat2j}$ mice. In male mice, we evaluated the shape, number of poles and misaligned chromosomes in both $Nek1^{+/+}$ (n = 100) and $Nek1^{kat2j/kat2j}$ (n = 100) spermatocytes. MI spindles from $Nek1^{+/+}$ spermatocytes showed a bipolar structure with the chromosomes aligned at metaphase plate (Fig 1a), while spindles from $Nek1^{kat2j/kat2j}$ spermatocytes showed defects in the structure of the spindle as well as in chromosome congression. These defects included MI spindles without a pole, with only one pole, with misaligned chromosomes (Fig 1b), and with multiple poles (Fig 1c). A total of 55% of spindles from $Nek1^{kat2j/kat2j}$ males were abnormal, while only 18% of the spindles from $Nek1^{+/+}$ male spermatocytes showed abnormalities (Fig 1d). Quantification of spindle abnormalities in $Nek1^{+/+}$ and $Nek1^{kat2j/kat2j}$ spermatocytes reveals that the most common abnormality is misaligned chromosomes. The percentage of spindles with misaligned chromosomes in $Nek1^{+/+}$ was 18%, while in $Nek1^{kat2j/kat2j}$ mice the percentage reached 38%. Other observed spindle abnormalities were absence of poles, one pole and multiple poles (Fig 1e)

The analysis of MI spindles in oocytes from $Nek1^{+/+}$ females showed a bipolar structure of the spindle and appropriate congression of the chromosomes at the metaphase plate (Fig 2a). However, MI spindles from $Nek1^{kat2j/kat2j}$ females showed a distortion of the structure of the spindle characterized by the presence of multiple spindles, mini spindles and misaligned chromosomes (Fig 2b, 2c and 2d) (for a complete analysis of the oocyte spindle dynamics, see S1 Fig). We evaluated the percentage of abnormal spindles in both wildtype oocytes (n = 100) and mutant oocytes (n = 100). In $Nek1^{kat2j/kat2j}$ female spindles, 82% of the MI spindles were abnormal, while only 22% of the $Nek1^{+/+}$ oocytes showed any abnormality (Fig 2e). Analysis of oocyte spindle defects showed that the most frequent defect is misaligned chromosomes: the number of oocytes with this defect 3.5 times higher in $Nek1^{kat2j/kat2j}$ (70 cells) compared to $Nek1^{+/+}$ oocytes (22 cells). No minispindles or mutipole spindles were observed in $Nek1^{+/+}$ oocytes. Besides the differences observed in the spindle phenotype in male and female, our results indicate that NEK1 is required for spindle formation during meiosis.

$Nek1^{ka2tj/kat2j}$ spermatocytes and oocytes have an abnormal spindle length and width

The appropriate length and width of the spindle are critical for establishing tension during segregation, and thus both parameters were evaluated them in male and female spindles. To perform this analysis in both male and female spindles we excluded all the cells that showed spindles without a pole, one pole, multipole, and minispindles, only those with two poles were evaluated. We measured the distance between poles in MI spermatocyte spindles and we observed a significant increase of the length of $Nek1^{kat2j/kat2j}$ males (27.9 μm ± 7.0 s.d.) compared to that of $Nek1^{+/+}$ males (23.1 μm ± 2.0 s.d.; Unpaired t test p = 0.0020; Fig 3a). Increases in MI spindle length in male spermatocytes were also accompanied with increases in the width in MI spindles from $Nek1^{kat2j/kat2j}$ male mice (26.7 μm, ± 6.4 s.d.) compared to that of $Nek1^{+/+}$ male mice (22.9 μm ± 2.1 s.d; Unpaired t test p = 0.0097; Fig 3b). We also analyzed the length and width of the female spindles. $Nek1^{kat2j/kat2j}$ oocytes showed an increase in the length of the spindle in MI oocytes (31.6μm ± 7.3 s.d.) compared to that found in $Nek1^{+/+}$ females (26.0 μm ± 2.3 s.d.; Unpaired t test p = 0.0007; Fig 3c). The lack of NEK1 also resulted in
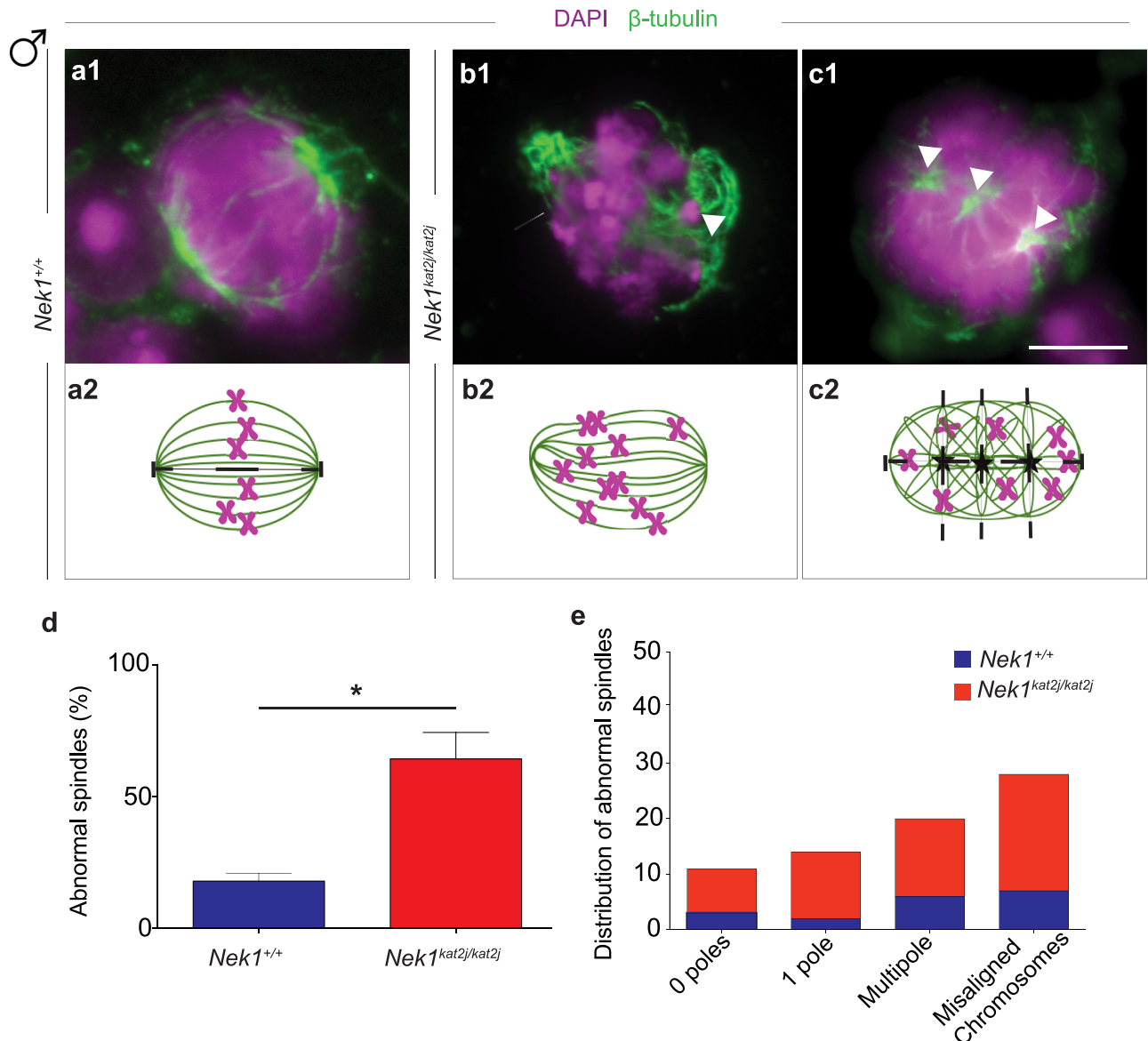
Fig 1. Loss of NEK1 results in disrupted spindle morphology and chromosome congression during meiosis I in spermatocytes.
(a-c) Immunofluorescence (IF) against β-tubulin (green) and DNA staining with DAPI (magenta) showing meiotic spindle morphology (panels a1-c1), with graphic representations below (panels a2-c2). (A) $Nek1^{+/+}$ spermatocyte shows normal spindle morphology and chromosome congression at the midplate of the spindle; (b, c) Examples of aberrant spindle morphology in spermatocytes from $Nek1^{kat2j/kat2j}$ mice showing monopolar spindles with mislocalized chromosomes resulting from failed chromosome congression (arrowheads) in b and multipolar spindles in c (arrowheads). (d) Quantitation of abnormal spindles in spermatocytes from $Nek1^{+/+}$ and $Nek1^{kat2j/kat2j}$ mice (n = 100 cells counted for each). (e) Quantitation cells with abnormal spindles by type of defect. Values are percentages ± Standard deviation. * Indicates statistically significant differences (Unpaired t-test $p < 0.05$).

altered width of the MI spindles in female meiosis. $Nek1^{kat2j/kat2j}$ oocytes showed a decrease in the width of the spindle (15.1 μm ± 4.0 s.d.) compared to the $Nek1^{+/+}$ oocyte spindles (17.0 μm ± 1.7 s.d.; Unpaired t test $p = 0.039$; Fig 3d). Taken together our results show that NEK1 is required for the establishment of the correct spindle length and width during meiosis in both male and female gametes.
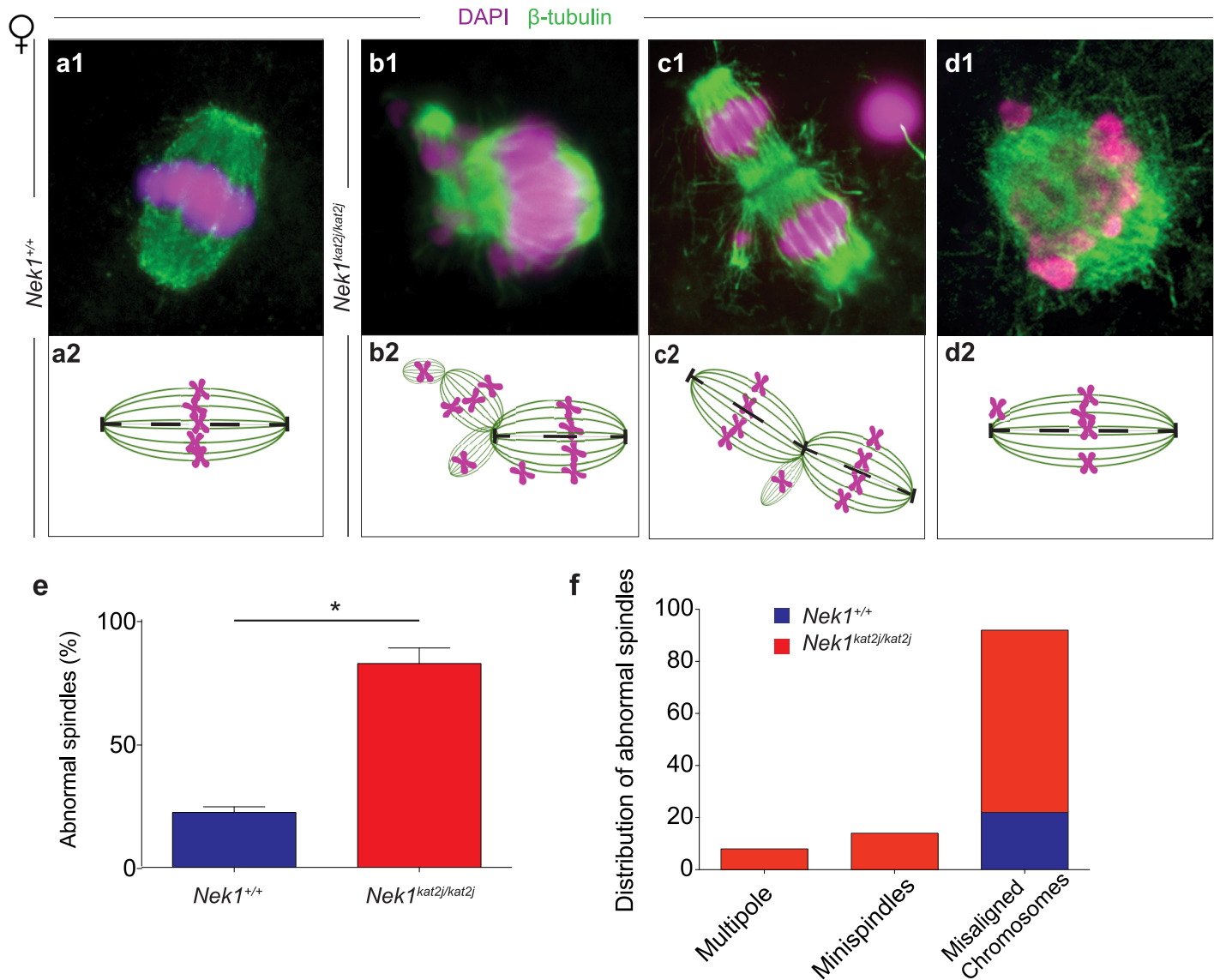
Fig 2. Loss of NEK1 results in disrupted spindle morphology and chromosome congression during meiosis I in oocytes. (a-d) Immunofluorescence (IF) against β-tubulin (green) and DNA staining with DAPI (magenta) showing meiotic spindle morphology (panels a1-d1), with graphic representations below (panels a2-d2). (a) $Nek1^{+/+}$ oocyte shows normal spindle morphology and chromosome congression at the midplate of the spindle; (b-d) Examples of aberrant spindle morphology in oocytes from $Nek1^{kat2j/kat2j}$ mice showing multipolar spindles with or without errors in chromosome congression (arrowheads indicate three extra spindles formed in the oocyte in b and two additional spindles in c). (e) Quantitation of abnormal spindles in oocytes from $Nek1^{+/+}$ and $Nek1^{kat2j/kat2j}$ mice (n = 100 cells counted for each). (f) Quantitation of cells with abnormal spindles by type of defect. Values are percentages ± Standard deviation. * Indicates statistically significant differences (Unpaired t-test p < 0.05).

Lack of NEK1 results in deregulation of myosin X (MYO10) and α-adducin (ADD1)

Given the disrupted spindle apparatus during meiosis I, we investigated possible protein targets of NEK1 to explain this phenotype. In a previous study, we had performed Mass spectrometry (MS) screening using testis protein extracts from $Nek1^{+/+}$ and $Nek1^{kat2j/kat2j}$ mouse [18]. Review of these data using GO terms for centrosome and centromeric proteins revealed no significant differences in these proteins levels in $Nek1^{kat2j/kat2j}$ mouse extracts compared to wildtype mice (S2 Fig). Several proteins associated with spindle formation and regulation were
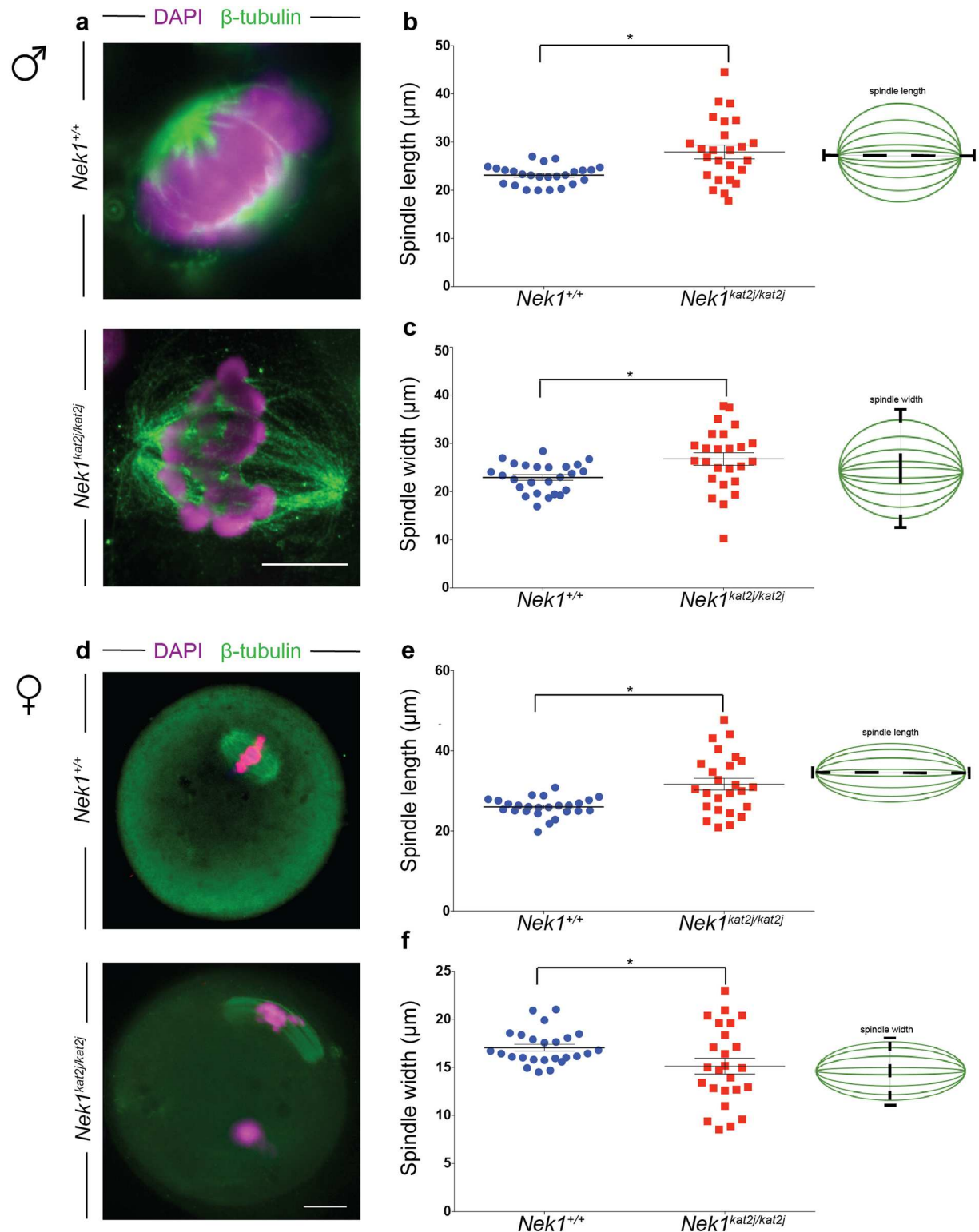
Fig 3. Lack of NEK1 results in abnormal meiosis I spindle morphology in spermatocytes and oocytes. (a) Immunofluorescence (IF) against β-tubulin (green) and DNA staining with DAPI (magenta) showing a wildtype (top) and *Nek1*^{kat2j/kat2j} spermatocytes (bottom), along with measurements of spindle length (b) and width (c). Black bars are means (μm) ± Standard deviation. (d) Immunofluorescence (IF) against β-tubulin (green) and DNA staining with DAPI (magenta) showing a wildtype (top) and *Nek1*^{kat2j/kat2j} (bottom) oocytes, along with measurements of spindle length (b) and width (c). Black bars are means (μm) ± Standard deviation. * Indicates statistically significant differences (Unpaired t-test p < 0.05).

identified and quantified, however no differences between $Nek1^{+/+}$ and $Nek1^{kat2j/kat2j}$ mouse were observed for tubulins, actins and SAC proteins (S3–S5 Figs).

Previous reports showed that MYO10 has a direct function in spindle formation [24–26]. In contrast to the tubulins, actins, and other spindle proteins that did not appear to be altered in the absence of NEK1, we observed that the levels of the myosins, MYO5, MYO7A, MYO10 and MYO15, were significantly increased in testis protein extracts from $Nek1$ mutant mice compared to wildtype littermates (S1 Table). By contrast, the myosins, MYO1B, MYO1C, MYO1D, MYO7A and MYO9B were unaltered. The function of MYO10 in spindle formation and integrity is related to its binding partner α-adducin (ADD1)[20]. Our MS results revealed that ADD1 showed lower protein levels in $Nek1^{kat2j/kat2j}$ male mice compared to wildtype male mice (S1 Table). The changes in protein levels observed by MS indicates that the loss of NEK1 results in an imbalance in the ratio MYO10/ADD1, and this could be affecting the proper spindle formation and function.

$Nek1^{kat2j/kat2j}$ spermatocytes and oocytes show aberrant localization of myosin X (MYO10) on meiotic spindles

We evaluated the localization of MYO10 on MI spindles from male spermatocytes and female oocytes. Immunofluorescence (IF) analysis in $Nek1^{+/+}$ spindles revealed that MYO10 localizes along the β-tubulin fibers specifically in mouse spermatocytes (Fig 4a). We analyzed the number of MYO10 foci per nucleus in the coronal plane (Fig 4b) and found an increase in the number of foci in the $Nek1^{kat2j/kat2j}$ mice (75.4 ± 6.7 s.d.) compared to $Nek1^{+/+}$ animals (66.3 ± 5.5 s.d.; Unpaired t test p = 0.0001). Analysis of transverse sections of male spindles revealed that there is a subtle accumulation of MYO10 at the spindle pole in $Nek1^{+/+}$ male mice (Fig 4a), and this was disrupted in $Nek1^{kat2j/kat2j}$ males (Fig 4b). In the transverse plane, we observed an increase in the MYO10 foci number in $Nek1^{kat2j/kat2j}$ mice (74.7 ± 5.4 s.d.) compared to the $Nek1^{+/+}$ mice (61.7 ± 4.4 s.d.; Unpaired t test p = 0.0001). The increase in MYO10 focus counts was supported by our mass spectrometry analysis showing increased MYO10 protein in testis extracts from $Nek1^{kat2j/kat2j}$ males compared to $Nek1^{+/+}$ mice (S1 Table).

We also evaluated the MYO10 foci in $Nek1^{+/+}$ oocytes (Fig 4c), where MYO10 localizes on tubulin fibers as foci during MI (39.7 ± 5.1 s.d.). In contrast to the situation in males, however, oocytes obtained from $Nek1^{kat2j/kat2j}$ females showed more small and dispersed foci that do not co-localize with β-tubulin. However, counts of MYO10 foci that co-localized with β-tubulin were significantly reduced (23.3 ± 5.4 s.d.; Unpaired T test p = 0.0001)(Fig 4d). This could indicate that the MYO10 is present but its capacity to bind to tubulin is reduced. Taken together, our results indicate that loss of NEK1 leads to mislocalization of MYO10 along meiotic spindles in both male and females germ cells, but that the regulation of MYO10 by NEK1 may be sexually dimorphic.

Localization of ADD1 on spermatocytes and oocytes is disrupted in absence of NEK1

Our previous MS results showed that ADD1 proteins levels are reduced in testis extracts from $Nek1^{kat2/kat2j}$ mouse compared to wildtype littermates (S1 Table)[18]. Thus, we evaluated the localization and protein levels of ADD1 in both male and female spindles during meiosis I. ADD1 localizes both to the poles of the spermatocyte spindles (Fig 5a, asterisk) and with β-tubulin fibers of the spindle (Fig 5a, arrow heads). We evaluated the ADD1 focus number associated with the spindle structure in coronal and transverse planes. MI spindles from $Nek1^{kat2j/kat2j}$ males showed a decreased ADD1 focus number (25.7 ± 7.8 s.d.) compared to MI spindles
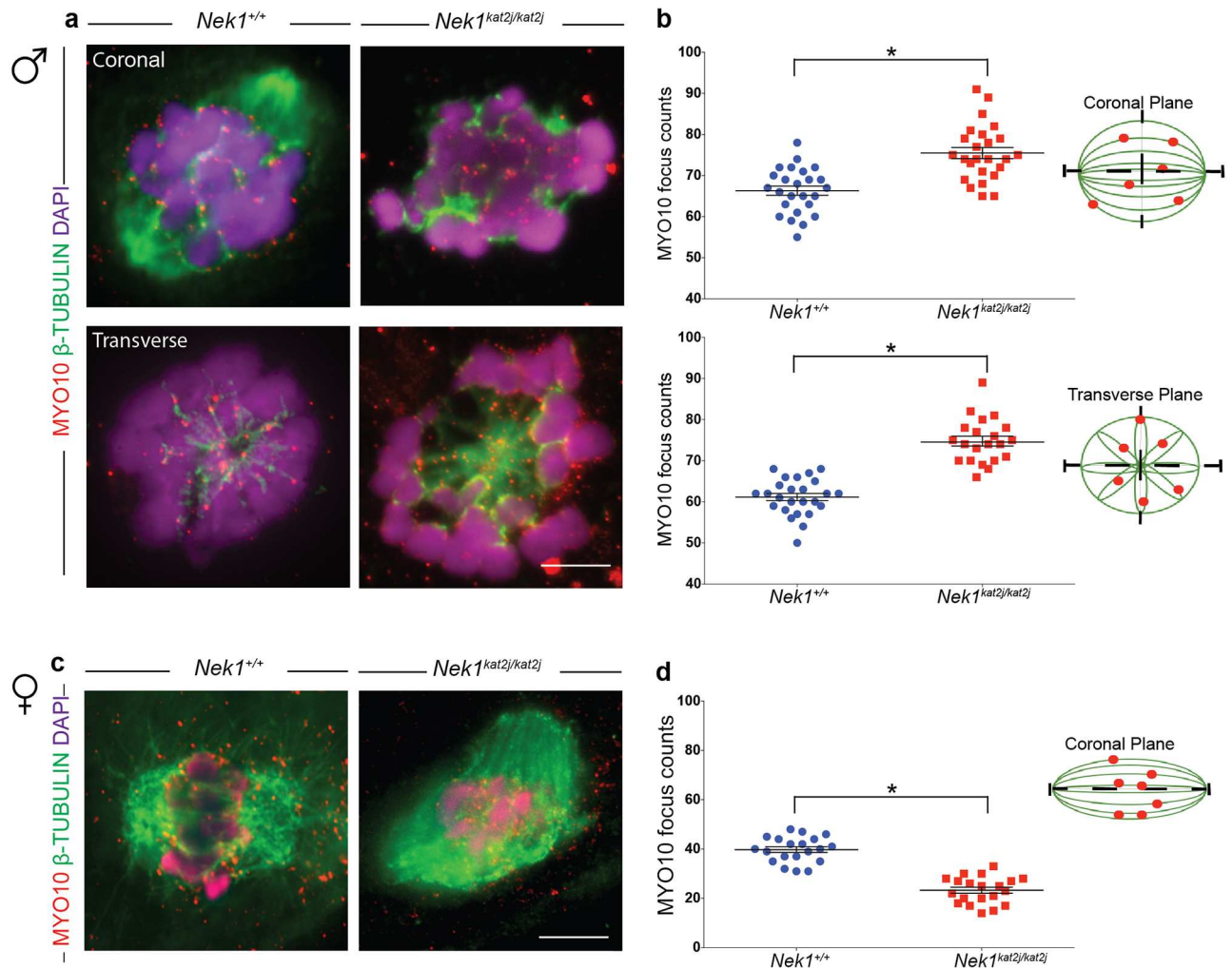
Fig 4. *Nek1^{kat2j/kat2j}* spermatocytes and oocytes show aberrant localization of myosin X (MYO10) on meiosis I spindles. (a) IF against MYO10 (red), β-tubulin (green) and DAPI (magenta) on spermatocytes from wildtype (left) and *Nek1^{kat2j/kat2j}* mice (right) in coronal (top) and transverse (bottom) planes. Arrowheads indicate examples of MYO10 foci. Quantitation of MYO10 focus counts per nucleus are given in panel (b). (c) IF against MYO10 (red), β-tubulin (green) and DAPI (magenta) in oocytes of both wildtype and mutant mice. Arrowheads indicate examples of MYO10 foci. Quantitation of MYO10 focus counts per nucleus are given in panel (d). All values are focus counts per spindle and black bars denote means ± Standard deviation. * Indicates statistically significant differences (Unpaired t test p < 0.05).

https://doi.org/10.1371/journal.pone.0185780.g004

from *Nek1^{+/+}* males (40.3 ± 3.2 s.d.), along with mislocalization of ADD1 on the spindle poles on the coronal plane (Unpaired t test p = 0.001)(Fig 5b). Analysis of the transverse plane of spindles from *Nek1^{kat2j/kat2j}* males showed a decreased focus number (32.6 ± 4.6 s.d.) compared to that of spindles from *Nek1^{+/+}* male (22.3 ± 5.5 s.d.; Unpaired t test p = 0.0001). Reduced ADD1 focus numbers were supported by reduced ADD1 protein levels analyzed by MS in testis extracts from NEK1 mutant mice and wildtype littermates (S1 Table). Thus, the effect of loss of NEK1 on ADD1 localization was the opposite to that seen for MYO10.

In oocytes from *Nek1^{+/+}* females, ADD1 also localized to the spindle poles as two large foci on each pole (3.6 ± 0.9 s.d.) (Fig 5c and 5d) (ADD1 signal along the tubulin fibers was observed but not quantified). This localization pattern was disrupted in *Nek1* mutant females, with elevated levels of ADD1 foci observed in the absence of NEK1. This was associated with the appearance of multiple foci on the poles (6.08 ± 1.4 s.d.; Unpaired t test p = 0.0002), rather
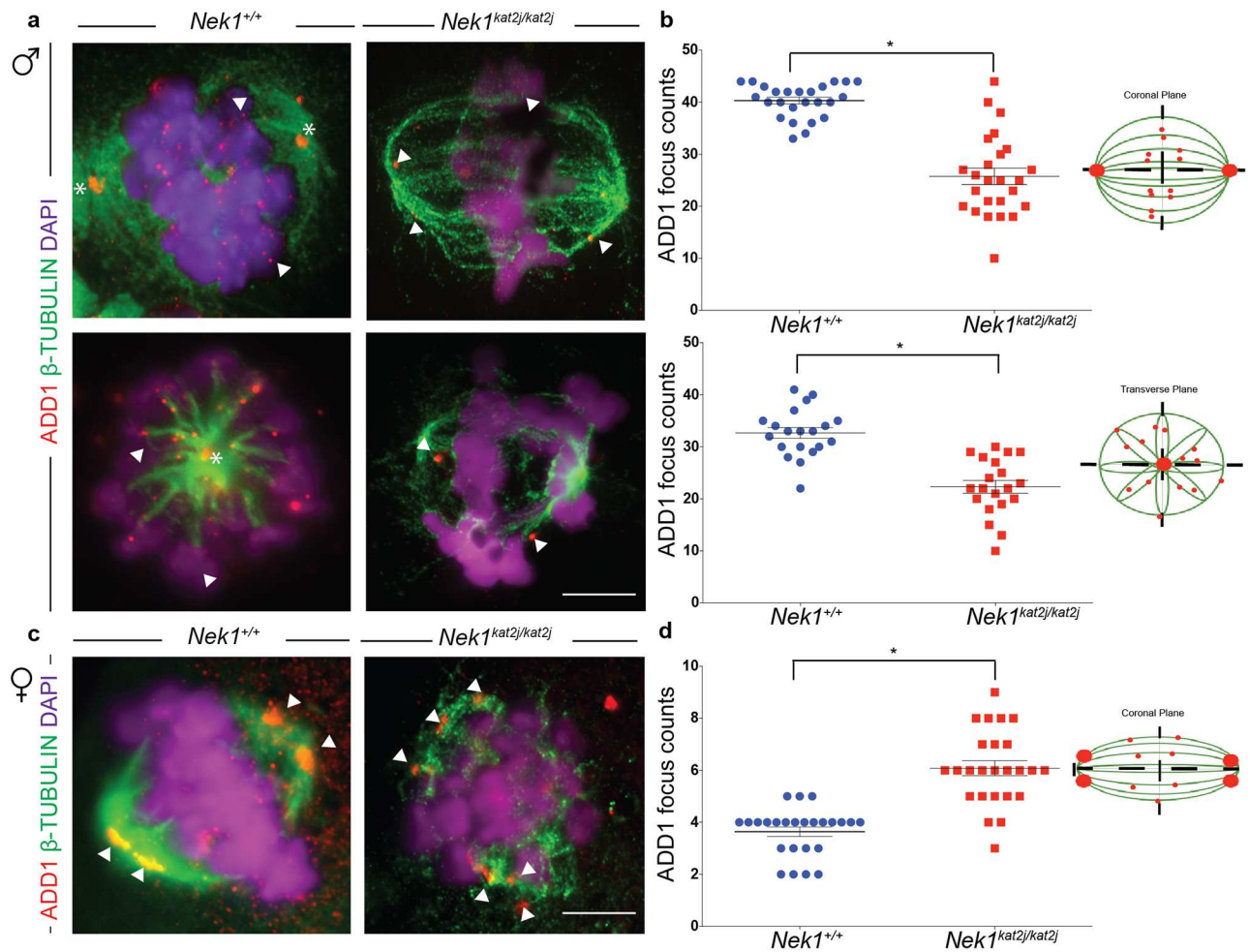
Fig 5. *Nek1^kat2j/kat2j* spermatocytes and oocytes show aberrant localization of Adducin 1 (ADD1) on meiosis I spindles. (a) IF against ADD1 (red), β-tubulin (green) and DAPI (magenta) on spermatocytes from wildtype (left) and *Nek1^kat2j/kat2j* mice (right) in coronal (top) and transverse (bottom) planes. Arrowheads indicate examples of ADD1 foci. Quantitation of ADD1 focus counts per nucleus are given in panel (b). (c) IF against ADD1 (red), β-tubulin (green) and DAPI (magenta) in oocytes of both wildtype and mutant mice. Arrowheads indicate examples of ADD1 foci. Quantitation of ADD1 focus counts per nucleus are given in panel (d). All values are focus counts per spindle and black bars denote means ± Standard deviation. * Indicates statistically significant differences (Unpaired t test p < 0.05).

than the two distinct large aggregations of ADD1. Again, as with the males, the change in ADD1 focus frequency on the meiotic spindles was the opposite to that seen for MYO10 (ADD1 foci increased on oocyte spindles in the *Nek1* mutant animals, whereas MYO10 foci decreased on oocyte spindles in the absence of NEK1). Taken together, these results demonstrate that loss of NEK1 alters the profile and ratios of ADD1 and MYO10 protein on meiosis I spindles in males and females, but that the effect may be sexually dimorphic.

Loss of NEK1 activity induces abnormal phosphorylation of ADD1

During mitotic spindle formation mammalian cell lines, ADD1 binds to the motor domain of MYO10 on the spindle. ADD1 and MYO10 interaction on mitotic spindles is negatively regulation by phosphorylation. Phosphorylation of ADD1 induces the loss of the interaction between both proteins and therefore the complex unloads from the mitotic spindle [20]. Phosphorylation of ADD1 results in abnormal mitotic spindle morphology (elongation, multipolar

spindles and aberrant chromosome alignment) and loss of its interaction with MYO10 [20]. We evaluated the proteins levels of ADD1 in testis lysates and isolated oocytes. Analysis of protein levels from testis lysates reveled a decrease in the protein levels in extracts from mutant mice compared to wildtype testis (Fig 6a; Unpaired t test p = 0.0031). We observed a clear double band in the $Nek1^{kat2j/kat2j}$ lysates, however this double band is not that obvious in the lysates from $Nek1^{+/+}$ testes. Decreased levels of ADD1 and the presence of a heavier band in WB analysis of $Nek1^{kat2j/kat2j}$ mouse compared to wildtype littermates suggested that the lack of NEK1 activity affects ADD1 phosphorylation. To test this hypothesis, we screened our previous phosphoproteomics data obtained from $Nek1$ mutant animals, specifically focusing on changes in ADD1. Loss of NEK1 results in a significant increase in the phosphorylation of ADD1, but not MYO10 (Fig 6b)[18]. Specifically, loss of NEK1 results in hyperphosphorylation of ADD1 on serine 465 (S465) (Fig 6c). Interestingly, ADD1 also showed an increase in deamidation of asparagine 462 (N462). Thus, both post-translational modifications could be acting as a trigger to induce the degradation of the protein.

The results described above show that the lack of NEK1 induces changes in spindle formation and protein localization in both spermatocytes and oocytes. However, the phenotype in both sexes is slightly different. We evaluated the relative protein levels of ADD1 in oocytes of both $Nek1^{+/+}$ and $Nek1^{kat2j/kat2j}$ oocytes. WB analysis revealed a decrease in ADD1 protein levels in $Nek1^{kat2j/kat2j}$ oocytes compared to $Nek1^{+/+}$ oocytes (Fig 6d; Unpaired t test p = 0.0003). As in male, GV oocytes from $Nek1^{kat2j/kat2j}$ mice showed a double band, however oocytes from $Nek1^{+/+}$ also showed a double band. In both wildtype and mutant, the slower migrating band had a stronger signal indicating that probably in oocytes the basal status of ADD1 is its phosphorylated state, at least at this stage of development. To evaluate the changes in the ADD1 protein levels according to oocyte maturation, we performed oocyte culture followed by WB. Our results showed that after 6h in culture, $Nek1^{+/+}$ oocytes showed the loss of the heavier band, possibly indicating a change in ADD1 phosphorylation. However in the $Nek1^{kat2j/kat2j}$ oocytes we observe that both bands almost disappear indicating that there is a change in the phosphorylation in the mutants but a faster degradation of the protein in the mutant oocytes. These results suggest that the phosphorylation levels of ADD1 in the mutant mice depends on active phosphorylation of the protein by a kinase that is mis-regulated in the absence of NEK1, or by loss of activity of a phosphatase that controls the phosphorylated status of ADD1. We previously reported the interaction of PP1γ with NEK1 and its function regulating the prophase pathway during meiosis [18]. To test if the changes of ADD1 phosphorylation similarly depends on PP1γ activity, we cultured $Nek1^{+/+}$ oocytes for 6h in the presence of the PP1γ inhibitor, Calyculin (Fig 6e). The WB analysis of these cultures showed that the inhibition of PP1γ induces a statistically significant increase in ADD1 protein levels, predominantly of the slower migrating band, suggesting that the inhibition of PP1γ maintains the phosphorylation status of ADD1. Thus, these results suggest that the lack of NEK1 action on ADD1 phosphorylation status may be the result of changes to PP1γ activity on ADD1.

Discussion

In eukaryotes, the structure orchestrating chromosome alignment and segregation during cell division is the microtubular spindle [3]. To ensure correct spindle dynamics, the spindle assembly checkpoint (SAC) becomes activated in situations where tension is not appropriately established between the chromosomes and the spindle poles, and this will block the progression of the cell cycle to prevent aberrant segregation. In addition to the canonical SAC, other levels of control have been described, including MYO10 [24–26]. In oocytes and frog embryos, disruption of MYO10 negatively affects nuclear anchoring and meiotic spindle formation [26],
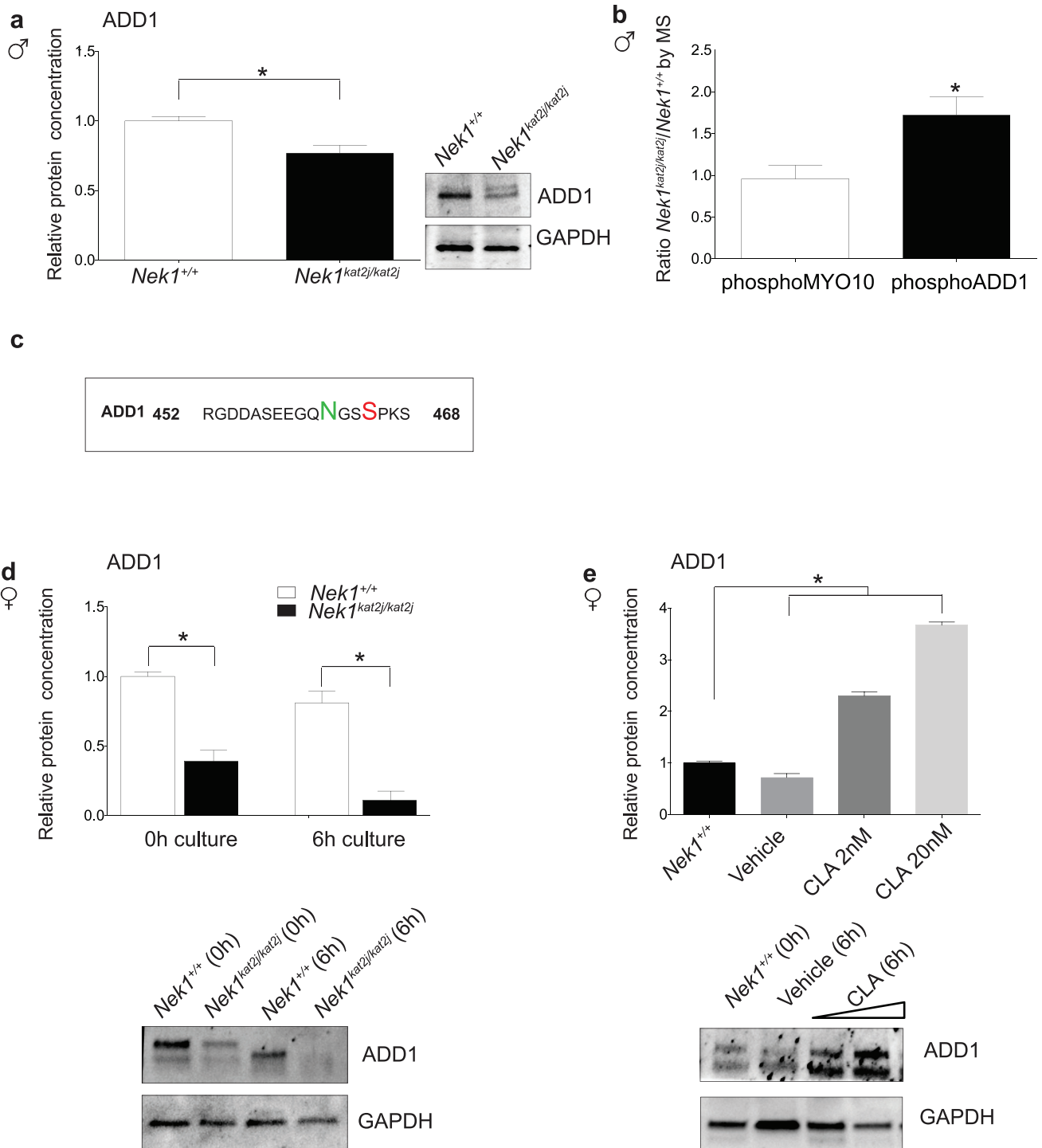
Fig 6. Loss of NEK1 during meiosis is associated with hyper-phosphorylation and reduced ADD1 protein in a PP1γ-dependent manner. (a) Quantitation of ADD1 protein levels in $Nek1^{+/+}$ testis extracts relative to GAPDH control. (b) ADD1 and MYO10 protein levels, expressed as a ratio of $Nek1^{kat2j/kat2j}$ / $Nek1^{+/+}$, as determined by mass spectrometry. (c) ADD1 phosphopeptide and deaminated peptide sequence determined by mass spectrometry to be higher in $Nek1^{kat2j/kat2j}$ testis extracts. (d) Quantitation by western blotting of ADD1 protein levels in oocytes at 0h and after 6h of culture. (e) Quantification of ADD1 protein levels in wildtype oocytes cultured for 6h in vehicle (ethanol) and the PP1 inhibitor Calyculin A (CLA) (at doses of 2 and 20 nM). All values are means ± Standard deviation. * Indicate statistically significant differences (Unpaired t test p < 0.05 and one-way ANOVA followed by Dunnett's multiple comparisons test, p < 0.05, for cultures with inhibitor)

https://doi.org/10.1371/journal.pone.0185780.g006

while depletion of MYO10 in frog epithelial cells induces abnormal spindle movements, spindle elongation, multi- spindle and pole fragmentation [25,27]. MYO10 has an amino-terminal globular head domain that harbors acting biding and ATPase activities, giving to the protein the capacity to bind F-actin. The tail of MYO10 has the MyTH4 and FERM domains that give to the protein the ability to interact with microtubules [26,28]. Accordingly, recent studies have demonstrated that loss of *Myo10* results in spindle dysfunction, while overexpression of only the MyTH4 domain alone affects the structure and shape of the spindle [24].

In the current study, we present evidence to suggest that loss of NEK1 induces increases in MYO10 protein levels in spermatocytes, and that this in turn may result in spindle defects. Our interpretation that overexpression of *Myo10* leads to spindle defects is in line with the suggestion that over-expression of the MyTH4 domain of MYO10 results in competition with the wildtype protein, leading to the displacement of the latter from the spindle [28]. Furthermore, it has been suggested that over-expression of only the MyTH4 may disrupt the functional link between F-actin, microtubules and MYO10. In our data (S1 Table), we observed an increase in the MYO10 protein levels without changes in F-actin or microtubules that could be inducing an imbalance in the protein levels provoking a similar phenotype to the overexpression of the MyTH4 domain. However, we could not eliminate the possibility that the lack of NEK1 could induce changes in other proteins or on the structure of MYO10 that induces mislocalization and/or abnormal function of MYO10. However, more studies using a MYO10 conditional knockout or siRNA against MYO10 will help to answer these possibilities.

ADD1 is an actin-biding protein that is important for membrane stabilization [29] and for cell-cell adhesion [30,31]. There are 3 isoforms of ADD with similar domain structures that are formed by NH$_2$-terminal head domain, a neck domain and a C-terminal domain. The C-terminal domain is characterized by it high contain of myristoylated alanine-rich C kinase substrate (MARCKS), this MARCKS related domain is necessary for its interaction with F-actin, spectrin, and calmodulin [28,32–34]. Previous studies in somatic cells showed that loss of ADD1 leads to a failure in mitotic spindle formation characterized by distortion, elongation, multipolar spindles and abnormal chromosome alignment [20]. Here, we show that loss of NEK1 leads to a reduction in ADD1 protein levels in spermatocytes, abnormal ADD1 distribution on the meiotic spindle of spermatocytes, and consequent disruption of spindle formation and integrity. These phenotypes observed in meiotic cells are highly reminiscent of the phenotypes observed in somatic cells lacking *Add1* [20].

ADD1 and MYO10 interact via the MyTH4 domain of MYO10, and this interaction is critical for the correct spindle formation and function in mitotic cells [20,25,26,28]. Interaction of ADD1 to MYO10 is dependent on phosphorylation whereby phosphorylation of ADD1 by cyclin-dependent kinase 1 (CDK1) enables ADD1 to bind MYO10 on mitotic spindle [20]. Depletion of ADD1 or changes in phosphorylation status results in abnormal mitotic spindles (elongation, multipolar spindles and aberrant chromosome alignment) [20]. In the absence of NEK1 we observe an increase in the phosphorylation of ADD1 at S465 and deamination of N462. Such modifications could induce premature loss of the ADD1-MYO10 interaction, first by altered phosphorylation of the protein and then via degradation of the protein as a consequence of the deamidation, similar to the phenotypes observed in somatic cells [20]. However, it is unclear what kinase is phosphorylating ADD1 during meiosis, since the increased phosphorylation in the absence of NEK1 suggests the up-regulation of a kinase that is itself regulated by NEK1 (either directly or indirectly). Clear candidates could be CDKs, however, our MS results did not show any significant change in the profile of CDK in the absence of NEK1, and specifically no differences in CDK1 indicating that increases in phosphorylation of ADD1 does not depend of CDK1 pathway. Alternatively, the increased phosphorylation of ADD1 could suggest the existence of a phosphatase that is inactivated by the loss of NEK1, allowing

the hyperphosphorylation of protein. We previously showed that in *Nek1* mutants, there is a down regulation and abnormal phosphorylation in whole testis lysate of PP1γ, and our results of oocyte cultures in the presence of a PP1 inhibitor suggest that the increase in ADD1 phosphorylation could be mediated by a similar mechanism.

Our results showed the disruption of the spindle, however some inconsistences between male and female gametes were observed. In both cases is clear that the lack of NEK1 is affecting ADD1 and MYO10, but the phenotype is slightly different. Thus, loss of NEK1 results in an increase in MYO10 localization on male meiotic spindles and a decrease in MYO10 localization on female meiotic spindles. Conversely, loss of NEK1 induces a decrease in ADD1 localization on male spindles, while in females the lack of NEK1 induces an increment in focus number but smaller in size, suggesting a disruption in the protein loading or acceleration in protein degradation. It is possible, therefore, that the increased focus count for ADD1 associated with the oocyte spindle reflects lower amounts of total protein per focus and/or fragmentation of the structures with which ADD1 is associating. This is supported by the different appearance of ADD1 foci in NEK1-deficient oocytes compared to wildtype oocytes. Another important difference in *Nek1*^{+/+} and *Nek1*^{kat2j/kat2j} oocytes compared to spermatocytes is the presence of a double band of ADD1 in the WB analysis, suggesting that in wildtype oocytes there is a basal phosphorylated state of ADD1. However the main difference between WT and mutant is that in the wildtype after culture the heavier band disappear but the lighter band still present while in the mutant both bands disappear indicating the instability of the protein in the absence of NEK1. Further analysis of ADD1 dynamics during oocyte meiosis will require proteomics analysis of thousands of mouse oocytes, in order to understand the distribution and status of spindle regulatory proteins in the presence and absence of NEK1.

Taken together, our data indicate that effect of NEK1 is sexually dimorphic with respect to spindle association of key spindle-related proteins, as is often the case in other aspects of meiotic regulation, including recombination, chromosome pairing and synapsis [6,35–37]. Our results showed, how the lack of NEK1 induced changes in both male and female spindle however the variation in the female phenotype could be related to how the spindle is formed. In males the spindle formation depend on the centrosomes. In mitotic cells, centrosome's functions are regulated by other proteins of the NEK family such as NEK2, NEK6, NEK7 and NEK9 that in the absence of NEK1 could be modifying the interactions and function of tubulins or myosins [38–40]. However, female spindle formation does not depend of centrosomes, thus a potential compensatory function of other NEK's during the spindle formation is not present; inducing the differences observed in the female phenotype. The broad spectrum of abnormal spindles in female *Nek1*^{kat2j/kat2j} oocytes, also could be associated to the "leakiness" of spindle check point in females [41]. Besides, differences observed in the phenotype, the lack of NEK1 ends up in male and female infertility [16,17].

In summary, we propose that the loss of NEK1 activity induces abnormal spindle formation through a mechanism mediated by the imbalance of MYO10 and ADD1. The decreases in ADD1 and it abnormal localization on the meiotic spindle is mediated by an increase its phosphorylation and deamination that leads to loss of interaction of MYO10 with ADD1. Taken together our results show the importance of NEK1 in the control of spindle formation during male and female meiosis.

Supporting information

S1 Table. Myosin proteins quantitation by mass spectrometry.
(DOCX)

S1 Fig. Dynamics of spindle formation in *Nek1^kat2j/kat2j* oocytes. (a-f) Immunofluorescence agaitns β-tubulin (green) and DNA staining with DAPI (magenta) showing the spindle dynamics in Nek1kat2j/kat2j oocytes. a) Germinal vesicle (GV); b) Germinal vesicle breakdown (GVBD); c) Prometaphase I (ProI); d and e) Metaphase I (MI); f) Telophase I (TeI). Scale bar 20μm
(EPS)

S2 Fig. Analysis of centromere and centrosomal protein ratio *Nek1^kat2j/kat2j*/*Nek1^+/+* by massspectrometry in whole testis lysates.
(EPS)

S3 Fig. Analysis of tubulins protein ratio *Nek1^kat2j/kat2j*/*Nek1^+/+* by massspectrometry in whole testis lysates.
(EPS)

S4 Fig. Analysis of actins protein ratio *Nek1^kat2j/kat2j*/*Nek1^+/+* by massspectrometry in whole testis lysates.
(EPS)

S5 Fig. Analysis of spindle assembly checkpoint protein ratio *Nek1^kat2j/kat2j*/*Nek1^+/+* by massspectrometry in whole testis lysates.
(EPS)

Acknowledgments

Author Contributions

Conceptualization: Miguel A. Brieño-Enríquez, J. Kim Holloway, Paula E. Cohen.

Data curation: Miguel A. Brieño-Enríquez, Stefannie L. Moak, Paula E. Cohen.

Formal analysis: Miguel A. Brieño-Enríquez, Paula E. Cohen.

Funding acquisition: J. Kim Holloway, Paula E. Cohen.

Investigation: Miguel A. Brieño-Enríquez, Stefannie L. Moak, J. Kim Holloway, Paula E. Cohen.

Writing – original draft: Miguel A. Brieño-Enríquez, Paula E. Cohen.

Writing – review & editing: Miguel A. Brieño-Enríquez, Paula E. Cohen.

References

1. Gray S, Cohen PE. Control of Meiotic Crossovers: From Double-Strand Break Formation to Designation. Annu Rev Genet 2016; 50: 175–210. https://doi.org/10.1146/annurev-genet-120215-035111 PMID: 27648641

2. Duro E, Marston AL. From equator to pole: splitting chromosomes in mitosis and meiosis. Genes Dev 2015; 29: 109–122. https://doi.org/10.1101/gad.255554.114 PMID: 25593304

3. Bennabi I, Terret ME, Verlhac MH. Meiotic spindle assembly and chromosome segregation in oocytes. J Cell Biol 2016; 215: 611–619. https://doi.org/10.1083/jcb.201607062 PMID: 27879467

4. Ohkura H. Meiosis: an overview of key differences from mitosis. Cold Spring Harb Perspect Biol 2015; 7.

5. McKim KS, Hawley RS. Chromosomal control of meiotic cell division. Science 1995; 270: 1595–1601. PMID: 7502068

6. Morelli MA, Cohen PE. Not all germ cells are created equal: aspects of sexual dimorphism in mammalian meiosis. Reproduction 2005; 130: 761–781. https://doi.org/10.1530/rep.1.00865 PMID: 16322537

7. Fry AM, O'Regan L, Sabir SR, Bayliss R. Cell cycle regulation by the NEK family of protein kinases. J Cell Sci 2012; 125: 4423–4433. https://doi.org/10.1242/jcs.111195 PMID: 23132929

8. Meirelles GV, Perez AM, de Souza EE, Basei FL, Papa PF, Melo Hanchuk TD, et al. "Stop Ne(c)king around": How interactomics contributes to functionally characterize Nek family kinases. World J Biol Chem 2014; 5: 141–160. PMID: 24921005

9. Oakley BR, Morris NR. A mutation in Aspergillus nidulans that blocks the transition from interphase to prophase. J Cell Biol 1983; 96: 1155–1158. PMID: 6339527

10. Letwin K, Mizzen L, Motro B, Ben-David Y, Bernstein A, Pawson T. A mammalian dual specificity protein kinase, Nek1, is related to the NIMA cell cycle regulator and highly expressed in meiotic germ cells. EMBO J 1992; 11: 3521–3531. PMID: 1382974

11. White MC, Quarmby LM. The NIMA-family kinase, Nek1 affects the stability of centrosomes and ciliogenesis. BMC Cell Biol 2008; 9: 29. https://doi.org/10.1186/1471-2121-9-29 PMID: 18533026

12. Hilton LK, White MC, Quarmby LM. The NIMA-related kinase NEK1 cycles through the nucleus. Biochem Biophys Res Commun 2009; 389: 52–56. https://doi.org/10.1016/j.bbrc.2009.08.086 PMID: 19699716

13. Patil M, Pabla N, Ding HF, Dong Z. Nek1 interacts with Ku80 to assist chromatin loading of replication factors and S-phase progression. Cell Cycle 2013; 12: 2608–2616. https://doi.org/10.4161/cc.25624 PMID: 23851348

14. Liu S, Ho CK, Ouyang J, Zou L. Nek1 kinase associates with ATR-ATRIP and primes ATR for efficient DNA damage signaling. Proc Natl Acad Sci U S A 2013; 110: 2175–2180. https://doi.org/10.1073/pnas.1217781110 PMID: 23345434

15. Chen Y, Chen CF, Chiang HC, Pena M, Polci R, Wei RL, et al. Mutation of NIMA-related kinase 1 (NEK1) leads to chromosome instability. Mol Cancer 2011; 10: 5. https://doi.org/10.1186/1476-4598-10-5 PMID: 21214959

16. Upadhya P, Birkenmeier EH, Birkenmeier CS, Barker JE. Mutations in a NIMA-related kinase gene, Nek1, cause pleiotropic effects including a progressive polycystic kidney disease in mice. Proc Natl Acad Sci U S A 2000; 97: 217–221. PMID: 10618398

17. Holloway K, Roberson EC, Corbett KL, Kolas NK, Nieves E, Cohen PE. NEK1 Facilitates Cohesin Removal during Mammalian Spermatogenesis. Genes (Basel) 2011; 2: 260–279.

18. Brieño-Enriquez MA, Moak SL, Toledo M, Filter JJ, Gray S, Barbero JL, et al. Cohesin Removal along the Chromosome Arms during the First Meiotic Division Depends on a NEK1-PP1gamma-WAPL Axis in the Mouse. Cell Rep 2016; 17: 977–986. https://doi.org/10.1016/j.celrep.2016.09.059 PMID: 27760328

19. Janaswami PM, Birkenmeier EH, Cook SA, Rowe LB, Bronson RT, Davisson MT. Identification and genetic mapping of a new polycystic kidney disease on mouse chromosome 8. Genomics 1997; 40: 101–107. https://doi.org/10.1006/geno.1996.4567 PMID: 9070925

20. Chan PC, Hsu RY, Liu CW, Lai CC, Chen HC. Adducin-1 is essential for mitotic spindle assembly through its interaction with myosin-X. J Cell Biol 2014; 204: 19–28. https://doi.org/10.1083/jcb.201306083 PMID: 24379415

21. Page J, Suja JA, Santos JL, Rufas JS. Squash procedure for protein immunolocalization in meiotic cells. Chromosome Res 1998; 6: 639–642. PMID: 10099877

22. Kotaja N, Kimmins S, Brancorsini S, Hentsch D, Vonesch JL, Davidson I, et al. Preparation, isolation and characterization of stage-specific spermatogenic cells for cellular and molecular analysis. Nat Methods 2004; 1: 249–254. https://doi.org/10.1038/nmeth1204-249 PMID: 16144087

23. Sun X, Cohen PE. Studying recombination in mouse oocytes. Methods Mol Biol 2013; 957: 1–18. https://doi.org/10.1007/978-1-62703-191-2_1 PMID: 23138941

24. Sandquist JC, Larson ME, Hine KJ. Myosin-10 independently influences mitotic spindle structure and mitotic progression. Cytoskeleton (Hoboken) 2016; 73: 351–364.

25. Woolner S, O'Brien LL, Wiese C, Bement WM. Myosin-10 and actin filaments are essential for mitotic spindle function. J Cell Biol 2008; 182: 77–88. https://doi.org/10.1083/jcb.200804062 PMID: 18606852

26. Weber KL, Sokac AM, Berg JS, Cheney RE, Bement WM. A microtubule-binding myosin required for nuclear anchoring and spindle assembly. Nature 2004; 431: 325–329. https://doi.org/10.1038/nature02834 PMID: 15372037

27. Kwon M, Bagonis M, Danuser G, Pellman D. Direct Microtubule-Binding by Myosin-10 Orients Centrosomes toward Retraction Fibers and Subcortical Actin Clouds. Dev Cell 2015; 34: 323–337. https://doi.org/10.1016/j.devcel.2015.06.013 PMID: 26235048

28. Hirano Y, Hatano T, Takahashi A, Toriyama M, Inagaki N, Hakoshima T. Structural basis of cargo recognition by the myosin-X MyTH4-FERM domain. EMBO J 2011; 30: 2734–2747. https://doi.org/10.1038/emboj.2011.177 PMID: 21642953

29. Anong WA, Franco T, Chu H, Weis TL, Devlin EE, Bodine DM, et al. Adducin forms a bridge between the erythrocyte membrane and its cytoskeleton and regulates membrane cohesion. Blood 2009; 114: 1904–1912. https://doi.org/10.1182/blood-2009-02-203216 PMID: 19567882

30. Abdi KM, Bennett V. Adducin promotes micrometer-scale organization of beta2-spectrin in lateral membranes of bronchial epithelial cells. Mol Biol Cell 2008; 19: 536–545. https://doi.org/10.1091/mbc.E07-08-0818 PMID: 18003973

31. Franco T, Chu H, Low PS. Identification of Adducin-Binding Residues on the Cytoplasmic Domain of Erythrocyte Membrane Protein, Band 3. Biochem J 2016.

32. Scaramuzzino DA, Morrow JS. Calmodulin-binding domain of recombinant erythrocyte beta-adducin. Proc Natl Acad Sci U S A 1993; 90: 3398–3402. PMID: 8475088

33. Kaiser HWO'Keefe E, Bennett V. Adducin: Ca++-dependent association with sites of cell-cell contact. J Cell Biol 1989; 109: 557–569. PMID: 2503523

34. Matsuoka Y, Hughes CA, Bennett V. Adducin regulation. Definition of the calmodulin-binding domain and sites of phosphorylation by protein kinases A and C. J Biol Chem 1996; 271: 25157–25166. PMID: 8810272

35. Herran Y, Gutierrez-Caballero C, Sanchez-Martin M, Hernandez T, Viera A, Barbero JL, et al. The cohesin subunit RAD21L functions in meiotic synapsis and exhibits sexual dimorphism in fertility. EMBO J 2011; 30: 3091–3105. https://doi.org/10.1038/emboj.2011.222 PMID: 21743440

36. Hayashi T, Kageyama Y, Ishizaka K, Kihara K, Oshima H. Sexual dimorphism in the regulation of meiotic process in the rabbit. Biol Reprod 2000; 62: 1722–1727. PMID: 10819776

37. Handel MA, Schimenti JC. Genetics of mammalian meiosis: regulation, dynamics and impact on fertility. Nat Rev Genet 2010; 11: 124–136. https://doi.org/10.1038/nrg2723 PMID: 20051984

38. Bertran MT, Sdelci S, Regue L, Avruch J, Caelles C, Roig J. Nek9 is a Plk1-activated kinase that controls early centrosome separation through Nek6/7 and Eg5. EMBO J 2011; 30: 2634–2647. https://doi.org/10.1038/emboj.2011.179 PMID: 21642957

39. Sdelci S, Schutz M, Pinyol R, Bertran MT, Regue L, Caelles C, et al. Nek9 phosphorylation of NEDD1/GCP-WD contributes to Plk1 control of gamma-tubulin recruitment to the mitotic centrosome. Curr Biol 2012; 22: 1516–1523. https://doi.org/10.1016/j.cub.2012.06.027 PMID: 22818914

40. Hames RS, Crookes RE, Straatman KR, Merdes A, Hayes MJ, Faragher AJ, et al. Dynamic recruitment of Nek2 kinase to the centrosome involves microtubules, PCM-1, and localized proteasomal degradation. Mol Biol Cell 2005; 16: 1711–1724. https://doi.org/10.1091/mbc.E04-08-0688 PMID: 15659651

41. Gorbsky GJ. The spindle checkpoint and chromosome segregation in meiosis. FEBS J 2015; 282: 2471–2487. https://doi.org/10.1111/febs.13166 PMID: 25470754